

**SBC2007-176454**

## **EFFECT OF HEAD POSTURE CHANGES IN THE GEOMETRY AND HEMODYNAMICS OF A HEALTHY HUMAN CAROTID BIFURCATION**

**Yannis Papaharilaou (1), Yiannis Seimenis (2), Nikos Pattakos (1), John Ekaterinaris (1),  
Georgios Georgiou (3), Elena Eracleous (2), Christos Christou (4),  
Brigitta C. Brott (5), Andreas Anayiotos (5)**

(1) Institute of Applied and Computational Mathematics, (2) Ayios Therissos Imaging Center,  
Foundation for Research and Technology-Hellas, Nicosia, Cyprus  
Heraklion, Crete, Greece

(3) Department of Mathematics and Statistics, (4) American Heart Institute,  
University of Cyprus, Nicosia, Cyprus Nicosia, Cyprus

(5) Department of Biomedical Engineering, University  
of Alabama at Birmingham, Birmingham, AL, USA

### **BACKGROUND**

Recent reports have stressed the importance of studying the morphology and hemodynamic changes of peripheral arteries in parts of the body that experience motion and posture change and their relationship to the hemodynamic hypothesis of atherosclerosis development [1, 2]. The carotid arteries may fall into this category since their geometric morphology and hemodynamic conditions may change due to head and neck posture changes. Such changes may alter the hemodynamic variables that are generally associated with the development of atherosclerosis, such as low and oscillating wall shear stress (WSS) and particle residence times. In this study, the carotid bifurcation of a healthy volunteer was imaged in the neutral position and in 3 different posture positions: a) flexion sideways to the right  $80^\circ$ , b) flexion upwards  $45^\circ$ , and c) flexion downwards  $45^\circ$  (Fig. 1). Anatomic and quantitative flow MR data were used to develop computational models to investigate the effect of different postures on arterial geometry and hemodynamic characteristics.

### **MATERIALS AND METHODS**

Using a 3.0 T Philips Achieva MRI instrument, a series of thin sequential slices were obtained by 3D TOF methods, covering the carotid artery bifurcation. The subject was scanned in the supine position using a head/neck phased array receiver coil. A 3D gradient-echo (GRE) pulse sequence (TE=3.5ms, TR=23ms, a flip angle (FA)= $20^\circ$ ,  $0.36 \times 0.36 \times 1.2 \text{ mm}^3$  acquisition and  $0.2 \times 0.2 \times 0.6 \text{ mm}^3$  reconstruction voxel) was employed. The inflow and outflow boundary conditions were obtained by MR phase contrast velocity mapping at the limits of the TOF covered anatomic region. Quantitative flow data were also obtained from two other locations inside the region of interest to serve as validation data for the numerical computations of the flow field using a 2D GRE sequence (TE=12 ms, TR=19 ms, FA= $10^\circ$ , Venc=65 cm/s,  $0.69 \times 0.69 \times 5.0 \text{ mm}^3$  acquisition and  $0.35 \times 0.35 \times 5.0 \text{ mm}^3$  reconstruction voxel). Peripheral pulse triggering was implemented and 30

temporal phases per RR cycle were obtained. Magnitude and phase-difference velocity-encoded images were derived using a view sharing reconstruction.

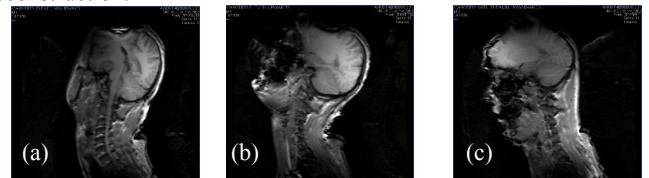


**Figure 1. The three head postures that were imaged (a)  $80^\circ$  flexion sideways, (b)  $45^\circ$  flexion upwards and (c)  $45^\circ$  flexion downwards**

Segmentation and 3D surface reconstruction of the MR images were implemented using purpose-developed software [3]. From the segmented MR images the 3D true vessel lumen surface was reconstructed. Abnormal, small scale surface irregularities introduced during the imaging and reconstruction processes applied were excluded from the computational model by applying pixel width constrained smoothing of the reconstructed surfaces prior to mesh generation. Smoothly matched cylindrical extensions of both inflow and outflow segments were added to facilitate the application of fully developed boundary conditions for the numerical simulation of the flow field. In order to quantify the effects of head posture on the 3D geometry of the carotid bifurcation we processed the reconstructed 3D lumen surface using VMTK [4] to extract the lumen centerlines.

Fluent v6.2 (Ansys Inc.) was used for the numerical computations of the carotid bifurcation flow field and Tecplot v.9 for post-processing the results. The computational grid was generated with ANSA (Beta CAE Systems, Thessaloniki, Greece). The computational domain was discretized using  $4.5 \times 10^5$  tetrahedral/pentahedral elements and non-uniform grid node spacing with higher grid density in the vicinity of the bifurcation was applied. Grid refinement was introduced by imposing a  $0.08 D$  (inlet diameter) viscous layer adjacent to

the wall in order to capture the steep gradients in the oscillating boundary layer. The arterial wall was assumed rigid and blood was assumed Newtonian and incompressible with a density of  $1.05 \text{ gr/cm}^3$  and a viscosity of  $4.5 \cdot 10^{-3} \text{ Pa}\cdot\text{s}$ . The CCA inflow waveform and the ICA-ECA flow split (0.65/0.35) were obtained *in vivo* by MR velocimetry. Based on the discrete Fourier series of the measured waveform, the exact Womersley solution was imposed at the inlet ( $Re_m=340$ ,  $\alpha=4.1$ ). The Oscillatory Shear Index (OSI) was computed as:

$$OSI = \frac{\int_0^T w |\boldsymbol{\tau} \cdot \mathbf{n}_m| dt}{\int_0^T |\boldsymbol{\tau} \cdot \mathbf{n}_m| dt}, \quad \mathbf{n}_m = \frac{1}{T} \int_0^T \left( \frac{\boldsymbol{\tau}}{|\boldsymbol{\tau}|} \right) dt, \quad w = 0.5(1 - \cos \alpha)$$

where  $\alpha$  is the angle between the shear vector  $\boldsymbol{\tau}$  and the time averaged mean shear direction  $\mathbf{n}_m$ . OSI varies between 0 for unidirectional shear flow and 0.5 for the purely oscillatory shear case.

## RESULTS

From the three postures that were imaged and simulated, the sideways flexion appeared to show significant changes in geometry as shown in Fig. 2. The other postures did not.

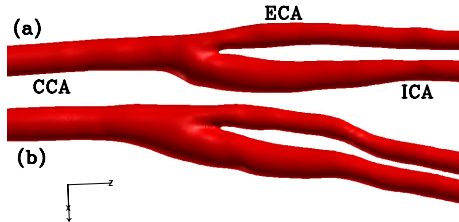


Figure 2. The carotid bifurcation geometry in the (a) neutral and (b) flexion rightways head posture

Curvature and tortuosity values were computed along the centerline. Geometric features of the carotid bifurcation such as the bifurcation angle, the asymmetry and planarity angles were also computed. Curvature values presented in Table 1 are averaged over the length of the CCA, ECA and ICA sections of the computed centerlines.

**Table 1. Comparison of 3D geometric features between carotid bifurcation models reconstructed from image sets obtained from the same subject but with different head postures**

		Neutral	Flexion rightways
	Bifurcation angle (deg)	29	34
	Asymmetry angle (deg)	11	2
	Planarity angle (deg)	4	4
CCA	Curvature (1/mm)	0.04	0.04
	Tortuosity	0.007	0.007
ICA	Curvature (1/mm)	0.02	0.04
	Tortuosity	0.005	0.005
ECA	Curvature (1/mm)	0.04	0.06
	Tortuosity	0.006	0.014

The information in Table 1 shows that there are indeed changes in the carotid bifurcation geometry caused by head posture. Certain geometric features appear more sensitive to the head position than others for the dataset studied. The bifurcation asymmetry angle drops dramatically in the flexion rightways case although the bifurcation angle remains almost the same. Tortuosity of the ECA and curvature of the ICA increase significantly. These changes influence the flow field. The computed time averaged streamlines in Fig. 3 show that flow

separation region is shifted upstream in the flexion rightways head posture as compared to the neutral head posture case. Fig. 4 (top) shows that for the flexed posture (b), regions of elevated OSI are augmented and the whole high OSI region is shifted upstream. To identify regions of low and oscillatory shear we consider a non-dimensional parameter which is calculated by dividing the OSI by the time averaged WSS magnitude normalized by the mean Poiseuille flow WSS ( $Re = 340$ ). When this parameter is considered, differences in the two cases are further accentuated, as illustrated at the lower panel in Fig. 4

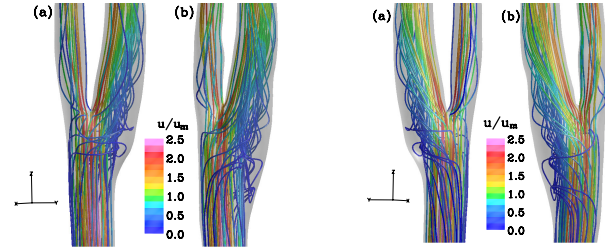


Figure 3. Numerically computed time averaged streamlines colored by time averaged normalized velocity magnitude of the carotid bifurcation with the head in the (a) neutral and (b) flexion rightways posture

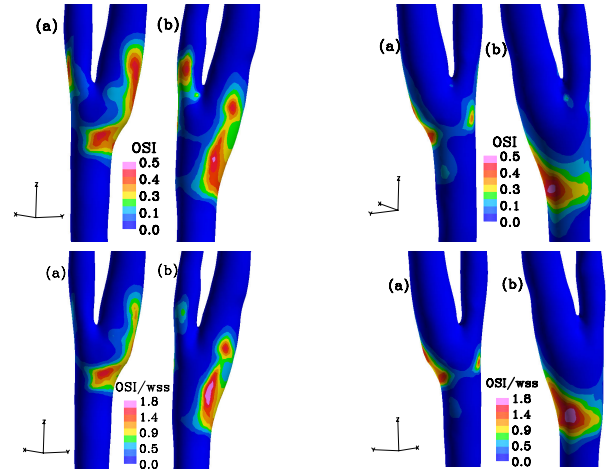


Figure 4. Numerically computed OSI (top) and OSI divided by normalized time averaged WSS magnitude (bottom) on the wall of the carotid bifurcation with the head in the (a) neutral and (b) flexion rightways posture

## CONCLUSIONS

Sideways flexion of the head may cause changes in the geometry of the carotid bifurcation which may influence the hemodynamic properties associated with the genesis, development and proliferation of arterial disease. Further research is warranted with more systematic clinical studies.

## REFERENCES

- [1] Steinman D.A. and Taylor C.A., 2005, *Ann Biomed Eng*, 33(12): 1704-1709.
- [2] Thomas J.B. et al., 2005, *Stroke*, 36(11): 2450-2456.
- [3] Giordana S. et al., 2005, *J Biomech*, 38(1): 47-62.
- [4] Antiga L. and Steinman D.A., 2004, *IEEE Trans Med Imaging*, 3(6): 704-713.

## ACKNOWLEDGMENT

The project was partially funded by a grant from the Cyprus Research Promotion Foundation.